energies

MDPI

Article

Complementarity between Combined Heat and Power Systems, Solar PV and Hydropower at a District Level: Sensitivity to Climate Characteristics along an Alpine Transect

Handriyanti Diah Puspitarini [1], Baptiste François [2], Marco Baratieri [3], Casey Brown [2], Mattia Zaramella [1] and Marco Borga [1,*]

1 Department of Land, Environment, Agriculture, and Forestry, University of Padova, 35020 Legnaro (PD), Italy; handriyantidiah.puspitarini@phd.unipd.it (H.D.P.); mattia.zaramella@unipd.it (M.Z.)
2 Department of Civil and Environmental Engineering, University of Massachusetts, Amherst, MA 01003, USA; bfrancois@umass.edu (B.F.); casey@engin.umass.edu (C.B.)
3 Faculty of Science and Technology, Free University of Bolzano, Piazza Università 5, 39100 Bolzano, Italy; Marco.Baratieri@unibz.it
* Correspondence: marco.borga@unipd.it

Received: 3 June 2020; Accepted: 4 August 2020; Published: 11 August 2020

Abstract: Combined heat and power systems (CHP) produce heat and electricity simultaneously. Their resulting high efficiency makes them more attractive from the energy managers' perspective than other conventional thermal systems. Although heat is a by-product of the electricity generation process, system operators usually operate CHP systems to satisfy heat demand. Electricity generation from CHP is thus driven by the heat demand, which follows the variability of seasonal temperature, and thus is not always correlated with the fluctuation of electricity demand. Consequently, from the perspective of the electricity grid operator, CHP systems can be seen as a non-controllable energy source similar to other renewable energy sources such as solar, wind or hydro. In this study, we investigate how 'non-controllable' electricity generation from CHP systems combines with 'non-controllable' electricity generation from solar photovoltaic panels (PV) and run-of-the river (RoR) hydropower at a district level. Only these three energy sources are considered within a 100% renewable mix scenario. Energy mixes with different shares of CHP, solar and RoR are evaluated regarding their contribution to total energy supply and their capacity to reduce generation variability. This analysis is carried out over an ensemble of seventeen catchments in North Eastern Italy located along a climate transect ranging from high elevation and snow dominated head-water catchments to rain-fed and wet basins at lower elevations. Results show that at a district scale, integration of CHP systems with solar photovoltaic and RoR hydropower leads to higher demand satisfaction and lower variability of the electricity balance. Results also show that including CHP in the energy mix modifies the optimal relative share between solar and RoR power generation. Results are consistent across the climate transect. For some districts, using the electricity from CHP might also be a better solution than building energy storage for solar PV.

Keywords: run-of-the river hydropower; solar power; combined heat and power; succeed indicators

1. Introduction

Heating and hot water are essential needs in many urban areas around the world. Private heaters and boilers fueled by energy sources generated in centralized locations (e.g., electricity, fuel oil or natural gas) are commonly used to satisfy these basic needs. District heating, on the other hand,

are systems within which heat and/or hot water are first generated in a centralized location, and then distributed to residential and commercial buildings through networks of pipelines, reducing in this way the need for in-situ generation through private heaters and boilers. Such systems have become more popular, especially with the growing installed capacity of combined heat and power (CHP) plants. For instance, Denmark and Finland, supply 75% of their district heating with CHP [1]. One explanation of the growing adoption of CHP technology is that it has the advantage of combining the generation of heat and electricity within a single process, which leads to higher overall efficiency [2,3].

Power generation from CHP plants for district heating is often considered as incidental since CHP are most of the time operated to supply heat and hot water first [4,5], although associated electricity generation can represent a significant share of the district supply. Using the example of Denmark, CHP power generation has represented 50% of the national electricity production [1]. At the scale of the European Union, CHP plants have supplied around 15% of the electricity demand, a share that is expected to increase to 22–25% by 2030 [6].

The usage of renewable energies, and more specifically of variable renewable energies (hereafter denoted as VRE) such as wind, solar, and hydro-power is widely considered for the replacement of conventional electricity production means [7–9]. A well-known challenge regarding the use of VRE sources for replacing conventional production means, however, relies on the variability and intermittency of VRE electricity generation, which would tend to significantly increase the dependence of the electricity generation and demand on weather and climate across a large range of temporal and spatial scales [10–12]. Despite substantial research showing the benefit of combining various VREs from local to continental scales (e.g., [13–20]), the need for storage or backup generation is acknowledged for balancing electricity generation from high shares of VRE with the demand [21,22].

Several studies investigated the potential of CHP plants to serve as back-up electricity generation for the VRE sources. For example, Söder et al. [23] reviewed the power production for the Nordic electricity market; and highlighted that in 2015 Denmark supplied 70% of its electricity demand by using a combination of wind power and CHP generation. Romero Rodríguez et al. [24] and Salmerón Lissén et al. [25] showed for a variety of climate conditions across Spain that a combined use of electricity generation from solar photovoltaic (PV) panels and cogeneration is a possible solution for reducing greenhouse gas at the building scale. Other research also provided multi-objective optimization approaches to optimize the use of CHP with other VRE sources while accounting for constraints associated with financial, environmental, and energy supply aspects (e.g., [5,26,27]). As several modeling frameworks have been proposed to address the question on the use of renewable energy sources combined with district-level CHP systems to further reduce greenhouse gas emissions and total system costs, the question of the sensitivity to climate variability on the complementarity between CHP and VREs is yet to be explored. François et al. [16] examined different combinations between solar PV, wind and run-of-river (RoR) hydropower energies across 12 regions in Europe and highlighted varying complementarity levels from Northern to Southern Europe. At smaller spatial scale, François et al. [15] also highlighted significant changes in complementarity between solar PV and RoR in Northeastern Italy; changes that could be explained from the change in hydrology regime with the elevation range. Such variability, mostly driven by the in-situ climate conditions, can either complicate or facilitate the combined use of VRE sources with other production means, such as CHP systems. Given this background, the objective of this study is to investigate how the integration of CHP with RoR and PV alters the overall electricity balance at the district level and to examine the sensitivity of this complementarity to the climate characteristics. Different heat penetration rates for CHP systems are considered within the districts, together with the use of storage capacity to balance generation with electricity demand. We use broadly accepted metrics to assess the complementarity among these energy sources; namely the demand satisfaction and the standard deviation of the electricity balance (defined as the deviation between supply and demand) [20].

To achieve this objective, we consider 17 districts located along a climate transect connecting the Alpine crests to the Veneto plain in Italy. This transect provides a range of climatic, environmental,

and ecological variability and it is of interest for three main reasons. First, it includes runoff regimes that gradually range from snow-melt dominated to rainfall dominated, with a ratio of solid to total precipitation decreasing from 0.6 in the northern part to almost 0 in the Veneto plain. François et al. [28] highlighted that this ratio controls the monthly correlation between RoR and solar power generation within this area, and thus the complementarity between the two VREs. Second, this region is characterized by a relatively high level of small RoR hydropower stations related to the initiatives of private actors or small communities. Third, the rate of PV equipment is rather high thanks both to public subsidies and easiness of installation [29]. Fourth, CHP plants provide the heat generation for the district heating network in this region [30].

The paper is organized as follows: Section 2 presents the analysis framework, including models of the CHP heat and electricity generation, the heat and electricity demand models, and the considered renewable sources and associated electricity generation. Section 3 describes the application to the Alpine transect. It includes the description of the study area and the data used for this application. Section 4 presents the results while Section 5 concludes and gives insights for future research.

2. Analysis Framework

The analysis framework aims at assessing the benefit of combining electricity generation from combined-heat power (CHP) plants operating within a district heating system, with electricity generation from other renewable energy sources. Two metrics are used to evaluate the benefit of CHP integration with other VREs: (i) the demand satisfaction and (ii) the standard deviation of electricity balance. The demand satisfaction is defined as the percentage of electricity demand that can be supplied by the system, giving insights on the temporal match between combined generation from different sources and the electricity demand, and as such the ability of the system to supply the load. The standard deviation of electricity balance is defined as the standard deviation of the difference between supply and demand, providing insights about the required balancing system costs for handling the remaining balance variability. This section describes the analysis framework that is considered for modeling electricity and heat generation from CHP, electricity and heat demand, electricity generation from the renewable energy sources (i.e., solar photovoltaic and run-of-the river power generation) and the electricity balance.

2.1. District Heat System and CHP Heat Generation

For a given urban or sub-urban area, we assume that CHP plants are primarily operated to supply heat demand through the district heating system. In locations where district heating system is not the only source for heat supply, CHP units are often operated to satisfy a given share of heat demand as follows:

$$H_{CHP} = H_s \cdot H_D, \quad (1)$$

where H_{CHP} (Wh) is the heat energy generated from the CHP plants within the district, H_D is the heat demand, H_s is the share of heat demand that is on average covered by H_{CHP}. Note that H_s can be larger than 1 if the district heating systems is oversized [31]. Conversely, $H_s = 0$ corresponds to an urban or sub-urban area that is not equipped with a district heating system. Due to its limited flexibility, heat generation from CHP plants is commonly kept constant for a given period and adjusted at a chosen frequency (e.g., monthly). Despite the variations of heat demand due to air temperature fluctuations at small temporal scales (e.g., hourly and daily), the heat demand can still be satisfied thanks to the thermic inertia of the district system [32,33]. This means that even though CHP heat generation at a given time is lower than the actual demand, supply can still be ensured by using the excess heat from a previous day for instance.

Time series of regional heat demand are often available at the country or regional level and at an annual time scale only. However, heat demand can be downscaled to district scale and to finer temporal resolution using the Heating Degree Day method [34]. The heating degree day (HDD) for

a given day j is defined as the sum of the positive deviations between the outdoor temperature and a temperature of comfort:

$$HDD(j) = \sum\nolimits_h (T_b - T_a(j,h))^+ \quad (2)$$

where $T_a(j,h)$ (°C) is the outdoor air temperature for the day j at the hour h; T_b is the temperature threshold below which space heat is needed in the buildings. Note that T_b is often set to 12 °C (e.g., [35,36]). The '+' symbol indicates that negative values within the brackets are set to 0. Following Ashfaq et al. [37], heat demand for the district and for a given day j can then be estimated from Equation (3):

$$H_D(j) = w{\cdot}p{\cdot}HDD(j), \quad (3)$$

where p is the number of inhabitants living within the district and w is a heat factor (Wh °C^{-1} inhabitant^{-1}). The heat factor w represents the marginal increment in heat demand per inhabitant and per degree Celsius that can be estimated from the observed total annual heat demand [37]:

$$w = \frac{\sum_{y,j} H_D(y,j)}{p{\cdot}\sum_{y,j} HDD(y,j)} \quad (4)$$

where y is a dummy variable for the specific years when observed annual heat demand is available.

2.2. Electricity Balance

The electricity balance is solved within the district considering the 100% renewable scenario, which corresponds to the scenario for which total electricity generation from various renewable energy sources within the district covers on average the electricity demand (Equation (5)):

$$\sum\nolimits_{i,j,h} E_i(j,h) = \sum\nolimits_{j,h} E_D(j,h) \quad (5)$$

where: $E_i(j,h)$ (Wh) is the total electricity generation from the sources i for day j and during hour h; E_D is the electricity demand within the district (Wh). Equation (5) is solved without accounting neither for the capacity of the electricity grid nor the losses that could occur at the level of the distribution grid within the district. This assumption is commonly referred to the copper grid assumption [38].

2.2.1. CHP Electricity Generation

The relationship between electricity generation and heat generation from a CHP plant differs from one technology to another (see [39] for a review of CHP technology). In this study, we consider the biomass-based CHP technology because it is the most common for district heating applications in the study area [40]). For this specific CHP technology, the ratio between the heat energy and the electric energy generation is kept constant and only adjusted at a seasonal basis depending on the heat demand in the district and the operator management strategy (Equation (6)):

$$E_{CHP}(j,h) = A(j){\cdot}H_{CHP}(j,h), \quad (6)$$

where H_{CHP} and E_{CHP} are respectively the heat and electric energy generated from the CHP plant for day j and hour h, and A is the power-to-heat ratio on day j [41]. This ratio is a decision variable for the plant operator who can decide to boost either heat or electricity generation during some period. It usually varies at seasonal scale. Because CHP plants are usually operated to supply heat demand first, the value of the power-to-heat is lower than 1.

2.2.2. Solar Photovoltaic Generation

Hourly solar photovoltaic (PV) generation is estimated from hourly air temperature T_a and hourly global horizontal irradiance (GHI) using the model defined by Equation (7) and adapted from [42]:

$$E_{PV}(j,h) = B \cdot GHI(j,h) \cdot (1 - \mu(T_a(j,h) - T_{C,STC}) - \mu \cdot C \cdot GHI(j,h)), \quad (7)$$

where μ and C are the solar panel temperature and radiation efficiencies, B is a constant parameter equal to the product between the invertor efficiency under standard test conditions (i.e., solar cell temperature $T_{C,STC}$ equal to 25 °C and solar irradiance equal to 1000 Wm^{-2}) and the surface covered by the solar panels (m^2).

2.2.3. Run-of-the River Hydropower Generation

Hydropower generation from run-of-river power plants depends on the water availability in the river network (Equation (8)):

$$E_H(j,h) = \eta_H \cdot g \cdot h \cdot \rho \cdot Q(j,h), \quad (8)$$

where $E_H(j,h)$ is electricity generation (kWh) during the day j at the hour h, η_H is the overall generator efficiency of the hydropower generation, Q is river flow that pass through the turbines ($m^3\ s^{-1}$), g is the acceleration of gravity ($m\ s^{-2}$), ρ is water density ($kg\ m^{-3}$), and h is the head (m). The volume of water that can be diverted from the riverbed to the power plant is limited by both environmental and technical constraints. The first constraint (Q_{min}) is a minimum water discharge that must remain in the riverbed to preserve the ecological continuity. The second constraint is represented by the design flow, i.e. the maximum water flow (Q_d) that can be diverted to the power plant, which depends on the existing infrastructure (e.g., the penstock and turbine capacity). The third constraint (Q_{max}) relates to the safety of the power infrastructure. When the river flow exceeds a given threshold, the safety of the power plant is threatened if it keeps running. To avoid any damages, the generation must be stopped. Common values for Q_{min}, Q_d and Q_{max} are 95th, 25th and 2nd percentiles of the natural flow, respectively [43,44].

Time series of river flows Q is required for assessing RoR power generation (Equation (8)). In this study, we use simulated rather than observed river flows to avoid the issue of missing data and gaps in time series. Using simulated streamflow has also the advantage to use data that is consistent for all the considered basins (both in terms of data quality and availability), which facilitates the comparison among the considered case studies. Note also that using hydrological simulations has been demonstrated to preserve well the complementarity between RoR power generation and solar PV generation in the studied region [44]. We use the integrated catchment hydrological model (ICHYMOD) to simulate hourly streamflow at the outlet of the considered catchments [45]. ICHYMOD is a semi-distributed rainfall-runoff that includes simulation of snow and ice accumulation and melt processes based on the version of TOPMELT presented by [46]. The simulation of surface and subsurface flows is carried out by means of the probability distribution model (PDM) from [47]. More detailed information about ICHYMOD is available in the Supplementary Materials of the article [48].

2.2.4. Electricity Demand Model

The demand for electricity varies seasonally, with higher demand during cold and hot days associated with usage of heating and cooling systems, respectively. It also varies significantly within a day, with low values commonly occurring at night and high values during daylight hours around noon and late afternoon. Daily demand for electricity is often modeled using the Temperature

Dependence Pattern (TDP, [49]) that uses a piecewise linear regression of the daily temperature to estimate electricity demand (Equation (9)):

$$E_D(j) = \begin{cases} a_{i,j,T_{Heat}} \cdot [T_{Heat} - T_a(j)] + b_{i,j} & if\ T_a(j) < T_{Heat} \\ b_{i,j} & if\ T_{Heat} < T_a(j) < T_{Cool} \\ a_{i,j,T_{Cool}} \cdot [T_a(j) - T_{Cool}] + b_{i,j} & if\ T_a(j) > T_{Cool} \end{cases} \quad (9)$$

where $E_D(j)$ is simulated electricity demand for the day j (Wh), T_a is air temperature, i and j are dummy variables refer to the day of the week (weekday, Saturday, Sunday, and holiday periods such as the summer and winter holiday seasons and some relevant religious celebration such as Easter). Simulated daily electricity demand $E_D(j)$ is then downscaled to hourly temporal scale $E_D(j,h)$ by means of a resampling approach described in [15].

2.2.5. Electricity Mix of CHP, Solar PV and RoR Power Generation

For a given share of heat supply H_s, the share of the electricity demand that is supplied by generation from CHP plants operating within the district is given by:

$$S_{CHP} = \frac{\sum_{j,h} E_{CHP}(j,h)}{\sum_{j,h} E_D(j,h)} = \frac{\sum_{j,h} A(j) \cdot H_{CHP}(j,h)}{\sum_{j,h} E_D(j,h)}. \quad (10)$$

Note that the share of the CHP electricity generation results from the share of heat demand H_s covered by the CHP plants within the district (Equation (1)). Given the case studies that are further described in Section 3, we here consider that solar PV and RoR power plants are operated within the district in addition to CHP power plants, even though the described methodology could be extended to other electricity sources such as wind or tidal energy sources, for example.

Given the 100% renewable scenario (Equations (5) and (11) below), the share of electricity demand covered by solar PV (S_{PV}) and RoR hydropower (S_{RoR}) power generation can then be defined by:

$$S_{PV} + S_{RoR} + S_{CHP} = 1. \quad (11)$$

The electricity generation from solar PV and RoR within a district is then given by:

$$E_{PV,district}(j,h) = S_{PV} \frac{\sum_{j,h} E_{PV}(j,h)}{\sum_{j,h} E_D(j,h)} \quad (12)$$

$$E_{RoR,district}(j,h) = S_{RoR} \frac{\sum_{j,h} E_{RoR}(j,h)}{\sum_{j,h} E_D(j,h)} \quad (13)$$

Note finally that $(1 - S_{CHP})E_D$ is the the residual demand to be supplied by solar PV and RoR. Defining the variable α as the share of the residual demand that is supplied on average by solar PV generation, the share S_{PV} and S_{RoR} can thus be rewritten such as:

$$S_{PV} = \alpha(1 - S_{CHP}) \quad (14)$$

$$S_{RoR} = (1 - \alpha)(1 - S_{CHP}) \quad (15)$$

The variable α, which ranges from 0 to 1, is further used to discuss the relative contribution from either solar PV or RoR hydropower for a fixed S_{CHP}.

2.2.6. VRE Storage

In addition to backup generation capacity, storage is used to balance temporal mismatches between electricity generation and demand. We here assumed that electricity generation from solar PV can be stored, for instance using batteries [50], which is a scenario very likely for the considered region:

$$S(t+1) = \begin{cases} \min[S_{max}, S(t) + (\eta_{in} \cdot \Delta(t))], & if\ \Delta(t) > 0 \\ \max[S_{min}, S(t) + (\eta_{out} \cdot \Delta(t))], & if\ \Delta(t) < 0 \end{cases}, \quad (16)$$

where S is the storage, S_{max} and S_{min} are the maximum and minimum capacities of the storage, η_{out} and η_{out} are the efficiencies of storage and power generation, and Δ is the difference between electricity demand and supply. For the sake of simplicity, we here assume a perfect storage with generation and storage efficiencies η_{out} and η_{out} both equal to unity. S_{min} is set to 0. A range of maximum storage capacity S_{max} is considered. It includes storage capacities that correspond to 3, 6, 12, 24, 48, and 72 h of hourly average demand. Electricity is stored when solar PV generation is larger than the demand and, inversely, stored electricity is released when generation from all available sources during the current time step is lower than the demand. The conventional operation strategy above-described is sometimes denoted as 'maximizing self-consumption strategy' [51]; other strategies exist such as the peak shaving strategy (see [52] for a comparison of different operating strategies). Note that operation of the storage capacity makes use of perfect foresight [53,54], which may lead to optimistic results compared to cases where uncertainty in weather and demand forecasts are accounted for (e.g., [55,56]), although the main conclusions of the study are expected to hold. More advanced storage models also exist and allow to better account for the physical constraints of the electrical storage, such as the decay in performance with aging (e.g., [57–59]).

3. Study Area and Data

The study area is represented by a climate transect connecting the Alpine crests to the Veneto plain in Italy (Figure 1). In this area, the share of heat demand covered by generation from CHP plants within the various district-heating systems is significant. For instance, in 2014, CHP power plants supplied the district heating systems more than 1050 GWh, which nearly corresponded to 25% of the regional heat demand [40].

The regional electricity demand is supplied by a combination of several production means and resources. Taking advantage of the elevation ranges and the above-average precipitation within the mountainous area, electricity generation from numerous hydropower plants (either dammed or run-of-the river power plants) supplies most of the regional electricity demand. Part of the electricity supply comes also from privately owned solar photovoltaic rooftop systems. Note that power capacity of rooftop PV systems is on the rise due to the increase of environmental concerns from both policy makers and public (cf. for example the C3-Alps project; http://www.c3alps.eu). Electricity generation from CHP plants used for district heating also contributes to supply. As an example, one of provinces in our study area, South Tyrol, covered roughly 10% of its electricity demand in 2014 using electricity generated from CHP [40]. According to the grid operator [60], the electricity production of CHP, hydropower, and solar power in Northeastern Italy in 2016 are 686.3 GWh, 9165 GWh, and 2319 GWh. Based on the above description, Northeastern Italy is an interesting study area that uses the high shares of VREs, and CHP plants for producing electricity and heat.

Within the study area, we specifically focus on a set of 17 districts, each one connected to a river basin for hydropower generation (Figure 1). We deliberately choose small basins with surface areas ranging from several km^2 to slightly less than 400 km^2 (Table 1). Focusing on small basins allows considering each basin as a potential urban or sub-urban district within which the balance between heat/electricity supply and the demand is solved using the analysis framework presented in Section 2. The location of the considered basins also allows exploring the sensitivity of the electricity balance to a range of climate conditions. Basins are indeed located at elevations ranging from slightly more

than 1000 m a.s.l. to more than 3000 m a.s.l. (Table 1). The variation of climate conditions with the elevation impacts the runoff regimes, with larger influence of snow accumulation and melt processes on streamflow in high elevation and larger influence of rainfall events at lower elevations (e.g., from convective systems during fall season). The interaction between elevation and the runoff regimes is illustrated in Table 1 via the ratio between snow and total precipitation (S/P ratio). High S/P ratio values (i.e., above 0.6) show a snowmelt dominated runoff regime while low S/P ratio values (i.e., below 0.4) indicates a rainfall-dominated regime. Runoff regimes at locations with intermediate S/P ratio values (i.e., in-between 0.4 and 0.6) are influenced by both snow accumulation and melt dynamics and by rainfall events.

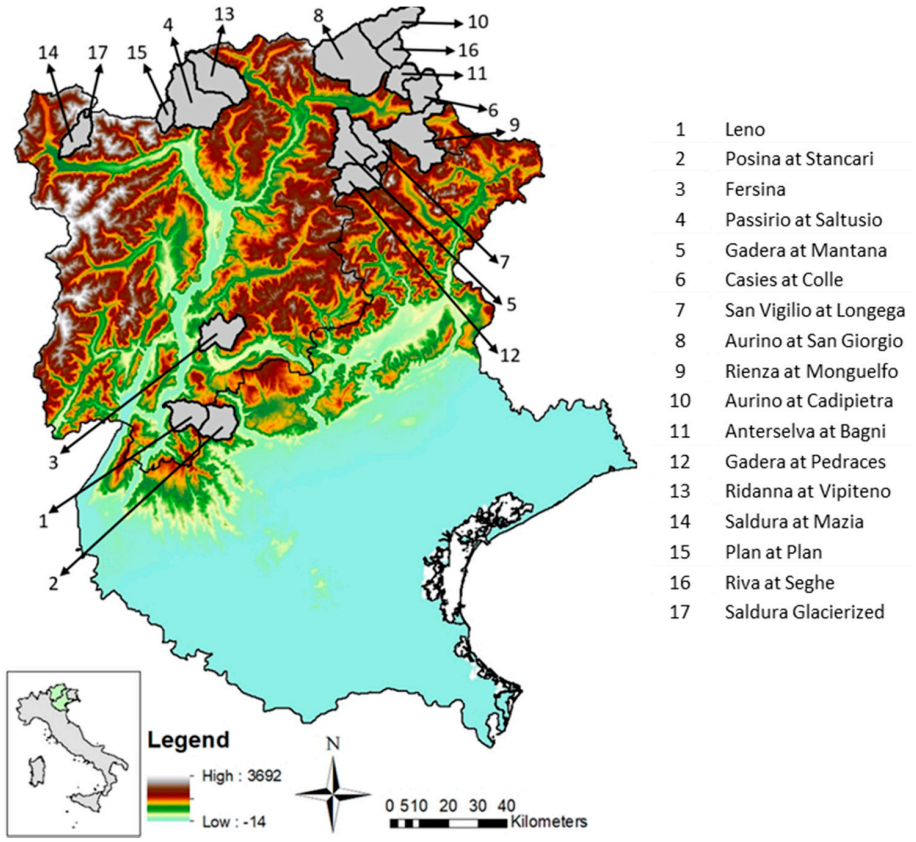

Figure 1. Map of the study basins in Italy.

Table 1. Main characteristics of the study basins. The basins are ranked (e.g., from 1 to 17) according to their ratio between solid precipitation and total precipitation (S/P ratio). A high S/P ratio indicates runoff regimes dominated by snow accumulation and melt while low S/P ratio indicates runoff regimes more dominated by precipitation events variability.

No	Basin Name	Area (km^2)	Mean Elevation (m a.s.l.)	S/P Ratio
1	Leno	113.0	1139.5	0.16
2	Posina at Stancari	116.0	1268.0	0.20
3	Fersina	138.0	1373.5	0.21
4	Passirio at Saltusio	292.2	1850.5	0.35
5	Gadera at Mantana	166.8	1882.5	0.36
6	Casies at Colle	117.0	1969.0	0.37
7	San Vigilio at Longega	103.7	1990.5	0.37
8	Aurino at San Giorgio	380.2	2077.5	0.48
9	Rienza at Monguelfo	264.5	2087.5	0.48
10	Aurino at Cadipietra	155.8	2156.0	0.52

Table 1. *Cont.*

No	Basin Name	Area (km^2)	Mean Elevation (m a.s.l.)	S/P Ratio
11	Anterselva at Bagni	82.7	2161.5	0.59
12	Gadera at Pedraces	124.9	2170.0	0.63
13	Ridanna at Vipiteno	204.6	2171.0	0.64
14	Saldura at Mazia	99.8	2309.5	0.72
15	Plan at Plan	49.8	2447.0	0.73
16	Riva at Seghe	78.9	2460.0	0.72
17	Saldura Glacierized	5.39	3116.0	0.86

The study is based on data that are either open source datasets available online or directly provided by local and regional environmental agencies. Given the temporal availability of the data, the analysis extends over a period of nine years ranging from 2000 to 2008. The analysis is carried out at hourly time resolution so that the daily cycles of electricity demand and solar PV electricity generation are accounted for.

Hourly temperature, precipitation and discharge data for the implementation and calibration of the hydrological model ICHYMOD were provided by the regional hydrological office. For modeling the demand for heat and hot water (Equation (3)), we use the total annual demand H_D for the year 2014 provided by EURAC [40]. Hourly air temperature T_a used for assessing the heating degree-day *HDD* (Equation (2)), solar PV generation (Equation (7)) and the electricity demand (Equation (9)) are ground observations mentioned above. We also assume that each basin (i.e., district) has a constant population p of 10,000 inhabitants. The hourly electricity consumption data used to calibrate the model are obtained from the European Network of Transmission System Operators of Electricity (ENTSOE, https://www.entsoe.eu/home/). Note that we use the model parameters calibrated by François et al., [15] for the study area. Hourly Global Horizontal Irradiation (GHI) data used for simulation of solar PV generation (Equation (7)) are reanalysis data available from the EXPRESS-Hydro database [61].

According to most common CHP plant specification in Trentino South Tyrol and Veneto regions, CHP are operated so that the power-to-heat ratio A varies at a seasonal basis (Equation (6)). During cold months (November through February), CHP electricity generation is low ($A = 0.15$) to prioritize heat generation. During summer months (May to August), CHP electricity generation is increased ($A = 0.45$) since heat demand is usually low at this season. For the rest of the year, the power-to-heat ratio takes an intermediate value ($A = 0.30$).

4. Results

4.1. Outlook of the Energy and Electricity Balance at the Districts Level

Figure 2 illustrates the heat and electricity demand and generation for Saldura at Mazia and Posina at Stancari districts under the 100% heat penetration scenario (i.e., $H_s = 1$). These two districts illustrate very distinct climate conditions within the study area. Saldura at Mazia is located at high elevation where winters are cold. Snowfall being the main source of precipitation at this elevation, runoff generation is mainly influenced by snowpack accumulation and melt dynamics.

On the other side of the transect, Posina at Stancari is located at lower elevation, temperatures are milder, and the influence of rainfall on the runoff regime dominates over snowmelt as the streamflow regime is more influenced by the occurrence of storms during spring and fall seasons. Due to its lower altitude, and thus higher average temperature, both heat and electricity demand for the Posina district are lower than for Saldura's. In both districts, heat demand shows larger seasonal variations than electricity demand. Because of the considered 100% heat penetration scenario (i.e., $H_s = 1$), heat generation varies at a monthly basis with monthly generation equal to the average monthly demand (Figure 2a). CHP electricity generation (Figure 2b) follows from the combination between the CHP heat generation pattern and the power-to-heat ratio (cf. Section 2.2.1). As a result, CHP electricity

generation is maximum during mild months as a tradeoff between mild air temperature and relatively high power-to-heat ratio.

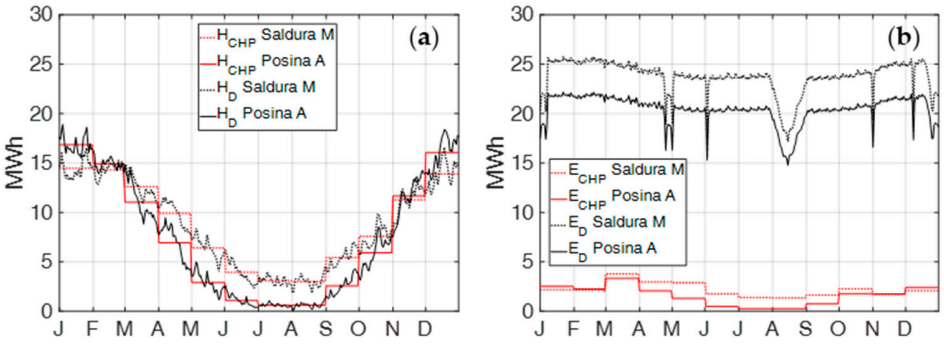

Figure 2. (**a**): Seasonal heat demand and CHP heat generation for the districts of Posina at Stancari (reported as Posina A, catchment #2 in Figure 1) and Saldura at Mazia (reported as Saldura M, catchment #14 in Figure 1). (**b**): Seasonal electricity demand and CHP electricity generation in Posina at Stancari and Saldura at Mazia. Note: the average cycles are obtained over the period 2000–2008. Heat demand values are smoothed by applying a 10-days moving window. Significant decreases in electricity demand follow from major holiday periods in Italy.

Figure 3 illustrates the daily and seasonal profiles of electricity generation and demand for the two-above districts. We note that solar PV generation is rather consistent across the two districts, which suggests a rather low impact of the elevation range on solar PV variability at both daily and seasonal scales. On the other hand, RoR hydropower generation profiles differ significantly from low to high elevations, which obviously results from differences in snowpack and glacier accumulation and melt dynamics that play a more important role at high elevation (e.g., [15,48]). For Saldura at Mazia, hydropower generation peaks during summer months (i.e., from mid-May to mid-September) when snow and ice melt rates are maximum. Besides this period, generation is low due to the winter drought period. Further South, at lower elevation where Posina at Stancari is located, RoR hydropower generation presents a completely different seasonal pattern as generation is low from mid-June through September and high during Spring and Fall seasons when intense precipitation and rainfall-over snow events are common and lead to moderate to high flows. CHP electricity generation patterns are rather similar at low and high elevations, although the seasonality is more pronounced at low elevation mainly due to warm temperatures in summer season that almost reduce heat demand to null values while demand can still be significant in high elevation at this season (Figure 2). At a seasonal scale, we retrieve the well-known result that generation variability is larger than electricity demand variability. Combining these different energy sources in the right proportion could thus help reducing the total generation variability and better match electricity demand.

4.2. Effect of CHP Integration on the Electricity Balance

The development of CHP within district heating systems is likely to affect the electricity demand satisfaction and the variability of the electricity balance. As detailed in Section 2, we assume that within the considered districts solar PV and RoR hydropower are, in addition to the incidental electricity generation from CHP plants, the two other sources for electricity. Considering the 100% renewable scenario defined by Equations (5), (11) and (14), an increase in CHP electricity generation (i.e., an increase in S_{CHP}) that follows from an increase in CHP heat penetration (i.e., an increase in H_s), replaces electricity generation from solar PV and RoR hydropower (i.e., decreases either S_{PV}, S_{RoR} or both). This section describes the effect of replacing solar PV and/or RoR power to CHP power generation while CHP heat penetration increases. Results are reported for the districts of Saldura at Mazia and of Posina at Stancari because these cases represent well the range of variability in the electricity balance.

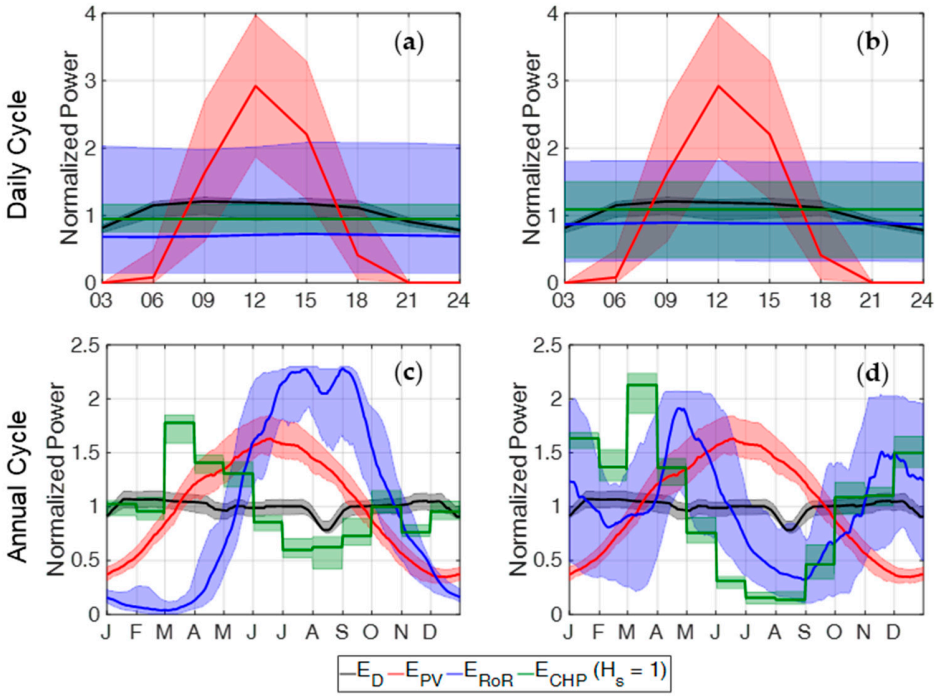

Figure 3. Daily (**a**,**b**) and annual (**c**,**d**) average cycles of solar PV (red), RoR hydropower (blue) and CHP (green) electricity generation, as well as demand (black), for the districts of Saldura at Mazia (**a**,**c**) and Posina at Stancari (**b**,**d**). Average cycles are obtained for the period 2000–2008. The shaded areas illustrate the sub-daily (top) and inter-annual (bottom) variability of the considered signal by showing the deviation between the 25th and 75th percentiles of their conditional distribution. Annual cycles are smoothed over a 10-day period. All cycles have been normalized (average = 1) to highlight the various patterns of demand and electricity generation at both temporal scales.

Figure 4 shows, as expected, that neither solar PV generation (α = 1) nor RoR hydropower generation (α = 0) alone maximizes the demand satisfaction or minimizes the electricity balance variability. Instead, combining solar PV and RoR power generation appears to be beneficial for the system. This result is consistent with previous studies that analyze the complementarity between PV and RoR hydro in Europe (e.g., [16]). We also note that when solar PV and RoR power generation is combined with the incidental electricity generation from CHP plants, demand satisfaction improves and the variability of the temporal mismatch between demand and total generation reduces. This mainly follows from the fact solar PV and RoR power plants have to be curtailed during peak generation around noon for solar PV and during the high flow seasons for RoR plants (cf. Figure 3). On the other hand, CHP electricity generation has low penetration, and so even for high CHP heat integration levels (Figure 2b and S_{CHP} coefficients in Table 2 that are almost always lower than 10%). As such, CHP generation is fully absorbed by the demand (i.e., no curtailment/loss of generation). Replacing solar PV and RoR power generation, which generates losses due to their significant variability, by CHP electricity generation that does not lead to losses even for high heat penetration, is thus an efficient way to maximize demand satisfaction for the same amount of generated electricity. For a given share between solar PV and RoR (i.e., for a given α coefficient), the increase in demand satisfaction (or decrease in electricity balance variability) appears to be a linear function of the CHP heat penetration (i.e., H_s coefficient). This is shown in Figure 4 as the curves of different colours are equally spaced. This result implies that, from an electricity balance standpoint, there is no drawback in integrating CHP power up to a heat penetration of 100% (i.e., $H_S = 1$).

Table 2. Effect of CHP integration on demand satisfaction, variability of the electricity balance and contribution from solar PV and RoR hydropower electricity sources. Results are shown for two districts with different climate conditions; Saldura at Mazia (S/P = 0.72) and Posina at Stancari (S/P = 0.20).

Basin	H_S Scenario	S_{CHP} (-)	S_{PV} (-)	S_{RoR} (-)	Demand Satisfaction (%)	Losses due to Temporal Mismatches (%)	Stdev Electricity Balance (-)
Saldura at Mazia (S/P = 0.72)	0	0.00	0.44	0.56	64.98	35.02	0.82
	0.2	0.02	0.43	0.55	65.70	34.3	0.81
	0.4	0.04	0.42	0.54	66.41	33.59	0.79
	0.6	0.06	0.42	0.53	67.12	32.88	0.77
	0.8	0.07	0.40	0.53	67.82	32.18	0.76
	1	0.09	0.39	0.52	68.53	31.47	0.74
	1.2	0.11	0.38	0.51	69.22	30.78	0.72
Posina at Stancari (S/P = 0.20)	0	0.00	0.31	0.69	73.87	26.13	0.62
	0.2	0.02	0.31	0.68	74.27	25.73	0.61
	0.4	0.03	0.30	0.67	74.67	25.33	0.60
	0.6	0.05	0.31	0.65	75.07	24.93	0.59
	0.8	0.06	0.30	0.64	75.46	24.54	0.59
	1	0.08	0.30	0.63	75.84	24.16	0.58
	1.2	0.09	0.30	0.61	76.21	23.79	0.57

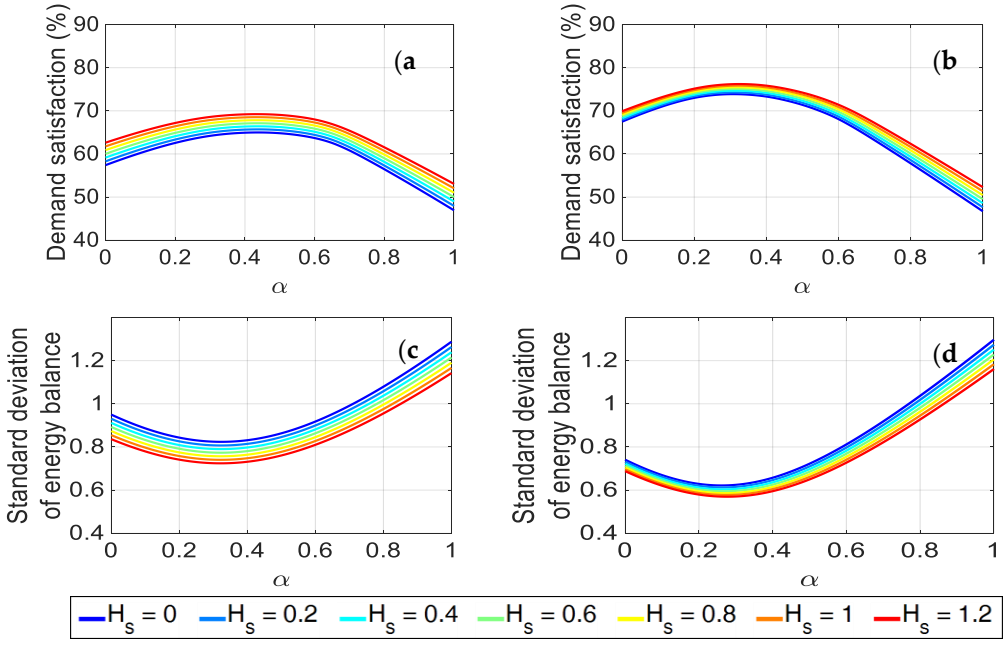

Figure 4. Demand satisfaction (**a**,**b**) and standard deviation of the electricity balance (**c**,**d**) as function of the share of solar PV generation (α) that covers the residual load $(1 - S_{CHP})E_D$. Note that the share of RoR hydropower generation is $(1 - \alpha)$. Results for Saldura at Mazia and for Posina at Stancari are reported in the left and right columns respectively. The various curves in color show changes in demand satisfaction and electricity balance variability as a function of the penetration level of CHP heat generation.

Figure 5 illustrates the change in demand satisfaction and electricity balance variability that results from integration of CHP ($H_s = 1$) with solar PV and RoR power along the climate transect shown in Figure 1. We note that districts located in snow-dominated catchments (i.e., high S/P values) benefit more from the integration of CHP plants than districts located in rain-fed catchments (i.e., low S/P values). This is both true in term of demand satisfaction (Figure 5a) and electricity balance variability (Figure 5b). This difference does not result from the balance at the hourly scale for which the generation patterns for each energy source are almost identical over both rain-fed and snowmelt dominated catchments (Figure 3). This result actually follows from the difference in complementarity at the seasonal scale between solar PV and RoR power generation in both climate areas. In snowmelt

dominated areas (i.e., high S/P values), because solar PV and RoR power are both maximum during summer months (Figure 3), the contribution from each energy source to the optimal mix is nearly even. RoR power has actually a slightly higher share than solar PV has (i.e., 56% and 44% respectively, Table 2) because its generation does not collapse to null values during the night and can thus supply demand during nighttime. This further means that, even for the optimal energy mix, a significant fraction of the generated power is lost (i.e., about 35%, Table 2). We note in Table 2 that when CHP plants are used within the district to supply heat demand, electricity from CHP replaces both solar PV and RoR power generation in proportion nearly equal. On the other hand, for districts located in rain-fed catchments (i.e., low S/P values), the initial complementarity between solar PV and RoR power is better. This can be observed looking at the seasonal patterns in Figure 3 or by comparing the demand satisfaction values in Table 2 for the scenario $H_S = 0$. In this case, the initial proportion of solar PV is significantly lower than the one observed for snowmelt dominated areas (i.e., 31%, Table 2), likely to prevent losses at both daily and seasonal scales. As a result, the integration of electricity from CHP plants mainly replaces RoR power generation, which, with a higher initial share (69%, Table 2), is more likely to lead to losses.

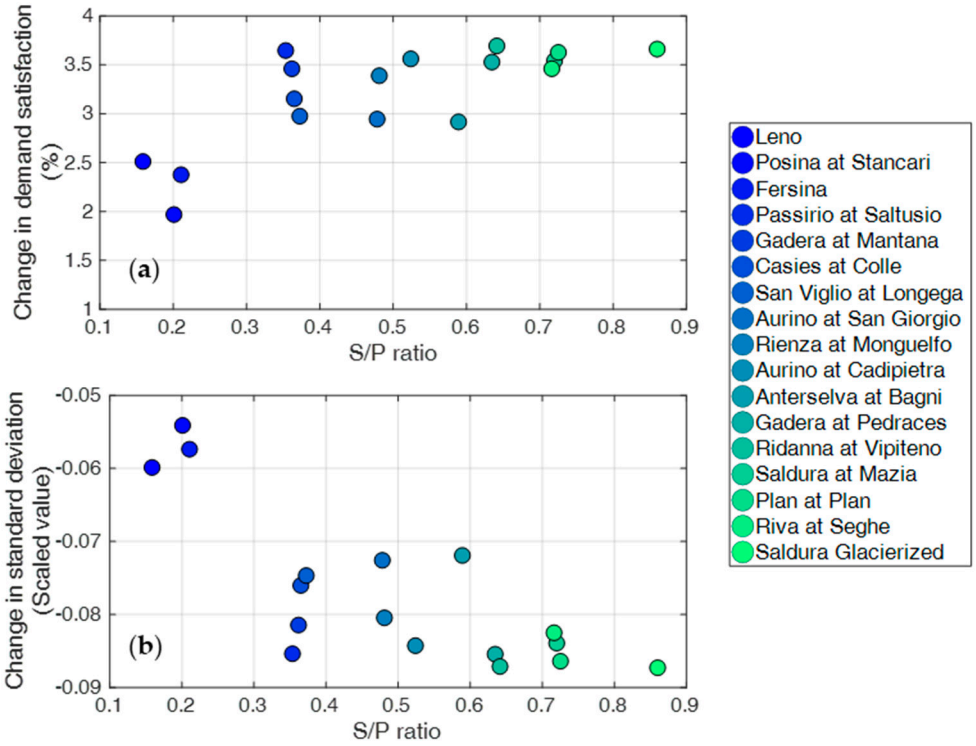

Figure 5. Change in electricity demand satisfaction (**a**) and electricity balance variability (**b**) when moving from an urban/sub-urban area with no district heating system ($H_s = 0$) to an area equipped with a district heating system covering 100% of the heat demand (i.e., $H_s = 1$). The considered districts are ordered according to their ratio between snowfall and total precipitation (S/P). The change in demand satisfaction is obtained by comparing the demand satisfaction (or the standard deviation of the electricity balance) for the best energy mix with or without CHP plants within the district (i.e., either $H_s = 0$ or $H_s = 1$).

4.3. Effect of Solar PV Storage in Addition to CHP Integration

Figure 6 illustrates the increase in demand satisfaction for Saldura at Mazia and Posina at Stancari heating districts ($H_S = 1$) when a storage capacity for solar PV is considered. By definition, the storage capacity for solar PV generation has no effect if the district only uses RoR power generation in addition to electricity from CHP plants (i.e., when $\alpha = 0$). Even for low shares of solar PV, the influence is not significant. This results from the fact that for low penetration levels (i.e., low α values), solar PV

generation is likely to remain below the load, which means no loss. However, if solar PV is the main source of electricity with CHP (e.g., value for α lager than 0.6), the increase in demand satisfaction is large for the first additional hours of storage capacity. The marginal increase in demand satisfaction for additional storage capacity above 12 to 24 h is then not significant, which highlights the fact that in-between 12–24 h of average load storage is enough to prevent the districts from losing most of the generated solar PV generation. This results clearly follows from the strong daily pattern for solar PV that dominates its seasonal pattern.

The influence of the storage capacity on the optimal share of solar PV slightly differs for the two considered districts. For Saldura at Mazia (Figure 6a), whether PV storage capacity is larger than 6 h, the share of PV that maximizes the demand satisfaction becomes $\alpha = 1$, which means that RoR is no more required in the mix. For Posina at Stancari (Figure 6b), the optimal share of PV is close to 0.6. Hence, even when a significant storage capacity is available for solar PV generation, the complementarity among RoR, Solar PV and CHP generation is such that RoR generation still benefits to the system.

The influence of PV storage capacity on the optimal demand satisfaction (i.e., the one obtained by using the optimal share for each electricity source) is illustrated in Figure 7 with and without a district heating system. As discussed previously, solar PV share increases significantly with PV storage capacity for the snowmelt dominated Saldura basin (i.e., up to 91%), while it barely gets larger than 56% for the rain-fed Posina at Stancari catchment. When CHP plants are integrated within the districts, PV storage above 6 h of average load capacity leads to the complete abandon of RoR power generation in the energy mix, while nearly 40% of RoR remain for rain-fed catchments, once again highlighting the better complementarity between solar PV and RoR plants in this climate area.

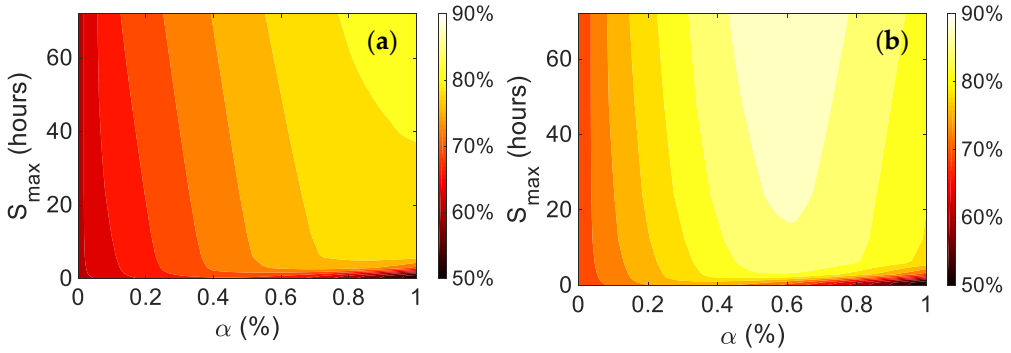

Figure 6. Influence of storage capacity available for solar PV (y-axis) on the electricity demand satisfaction (color map) as a function of the share between solar PV and RoR power generation within the mix (x-axis). Results are shown for Saldura at Mazia (**a**) and Posina at Stancari (**b**) and are obtained for a CHP heat penetration level $H_s = 1$, which correspond to CHP electricity share $S_{CHP} = 0.09$ and $S_{CHP} = 0.08$, respectively.

When comparing the demand satisfaction with and without CHP for different solar PV capacity (Figure 7), we note that whatever the storage capacity, CHP integration always increases the demand satisfaction. The larger increase associated with the integration of CHP within the district located in snowmelt dominated catchments (see discussion in Section 4.2) tends to be become similar to the one obtained for rain-fed catchments as soon as PV storage gets larger than 1 day of average load storage.

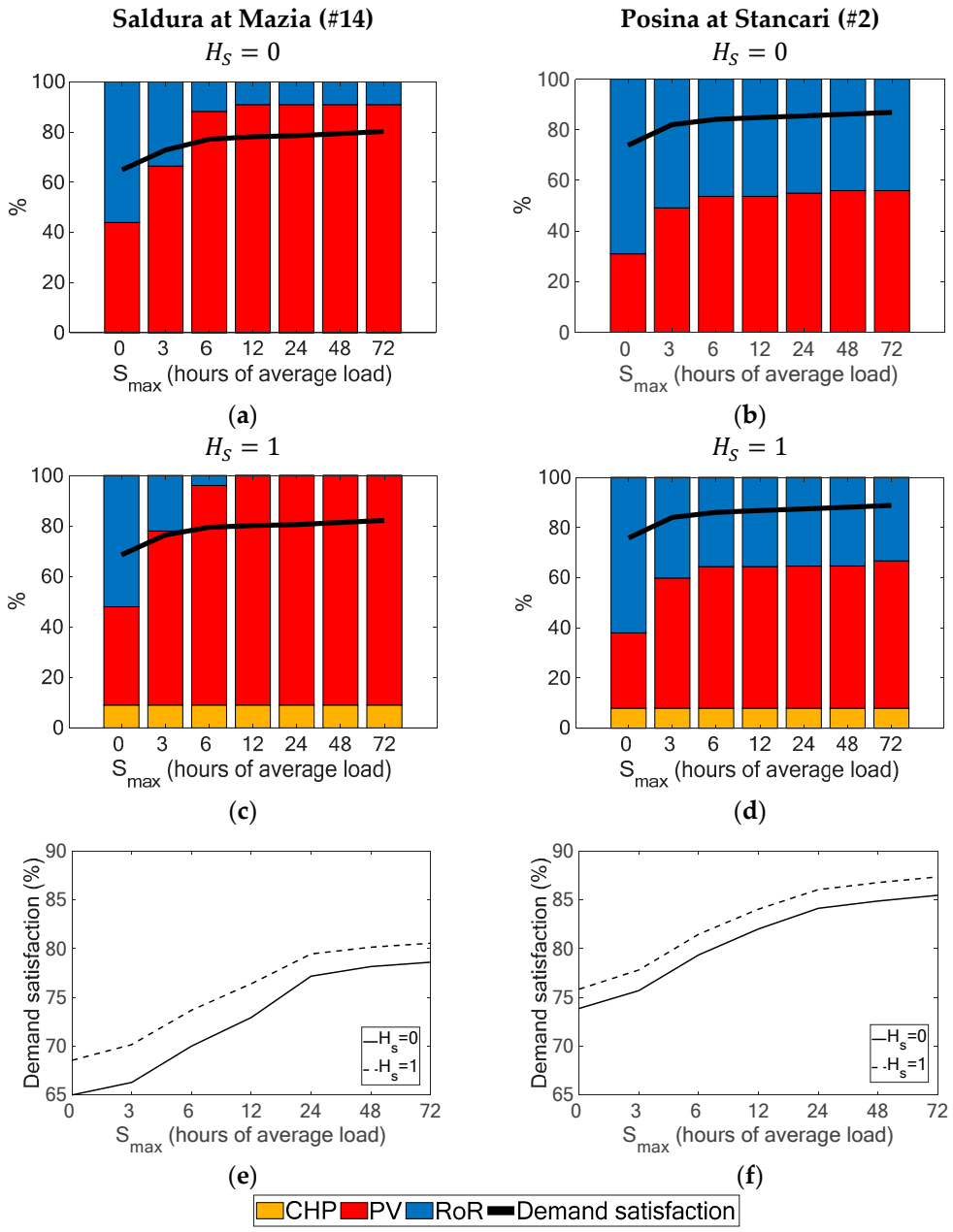

Figure 7. Influence of PV storage capacity (*x*-axis) on demand satisfaction (black line, %) and on the optimal mix combination between solar PV and RoR (**a**,**b**) and solar PV, RoR and CHP (**c**,**d**). The color bars show the share (%) of each electricity source. The third rows compare the demand satisfaction with and without CHP plants within the districts. Results are shown for Saldura at Mazia (**a**,**c**,**e**) and for Posina at Stancari (**b**,**d**,**f**).

5. Conclusions

District heating systems become more common worldwide with the development of CHP technology. Although driven by the heat generation, CHP electricity generation can provide a low fluctuating base generation that could reduce the need for variable renewable capacity. This study investigates this scenario by combining at the district level CHP electricity generation with both solar PV and RoR hydropower generation. The results show that the integration of CHP electricity reduces the variability of the electricity balance and increases the demand satisfaction; and this for all the considered locations along a climate transect in the Northeastern Italian Alps.

The integration of CHP plants within a district may modify the optimal contribution from solar PV and RoR power generation. These modifications are more significant for basins where runoff generation and associated RoR power generation are dominated by the intermittency of rainfall events. For these districts, the electricity from CHP tends to replace more generation from RoR generation for which the seasonal patterns are less complementary to match the electricity demand (Figure 3).

It is also interesting to highlight that for districts with installed solar PV storage capacity, using CHP plants represent a better solution for increasing further the demand satisfaction than allocating more storage. For instance in Figure 7, when comparing the demand satisfaction for Posina at Stancari with or without CHP, one notes that a system with CHP and 12 h of solar PV storage provides a similar demand satisfaction as a system without CHP but with double solar PV storage capacity (i.e., 24 h).

The conclusions of this research stem from the use of a simulated-based modeling framework that relies on four main assumptions. First, the modeling framework is free from constraints associated with the electricity grid (i.e., no loss and no transmission constraint capacity . . .). This assumption is often referred to the copper plate assumption (see [38]). Second, we use the 100% renewable energy scenario assuming that generation from the various sources covers on average the electricity demand over the considered period. Third, we use perfect foresight assumption for operating the electrical storage capacity. These assumptions have been broadly used on the complementarity literature (e.g., [13–15,19,38,48,53,62,63]) and none is expected to significantly influence the assessment of the sensitivity of the complementarity between CHP and solar PV/RoR hydropower described in this study. A fourth assumption/configuration used in this study concerns the relatively large, although limited, flexibility of the CHP electricity generation. This assumption could limit to some extent the generalization of the conclusions of this research to different types of CHP systems, which is the relative large, although limited, flexibility of the CHP electricity generation. While CHP systems are capable of fluctuate their heat/electricity generation, for instance at a monthly basis as described in Figure 2, such a flexibility is often not used in practice (e.g., [31,64]). However, some recent research (e.g., [54]) suggests that adapting the CHP systems would ease a more flexible use of CHP systems to eventually account for VRE generation and/or variable demand, which aligns well with the research effort described in our study.

Several future works should follow this research. For instance, our results are based on a single CHP technology (i.e., biomass) while other technologies with different constraints in their operations could provide different results. While the current operations of the considered CHP plants (i.e., power-to-heat ratio) have been chosen regarding the heat demand, they could be optimized to increase even more the electricity demand satisfaction, while solar PV and RoR power losses could be in turn used to generate heat via individual heating system. While our results suggest that using CHP could be a viable option to limit the requirement in electricity storage, evaluation of the costs associated to each technology is a critical step for further design guidance development. For doing so, the use of multi-objective optimization approach could be considered, for instance to maximize generation from renewable and CHP while accounting for the uncertainty in generation and demand, while minimizing the total system costs (e.g., [65–67]). Finally, the assessment of the robustness of the above conclusion within a climate change context would also be interesting, especially since heat demand is likely to decrease in the future warmer climate. As a result, CHP plants operators could increase electricity generation at the expense of heat generation. Such a change in the operations of the CHP plants would modify the temporal patterns of CHP electricity generation, and thus its complementarity with other energy sources.

Author Contributions: Conceptualization, H.D.P., B.F., and M.B. (Marco Borga); methodology, H.D.P., B.F., and M.B. (Marco Borga); software, H.D.P., M.Z., M.B. (Marco Borga); validation, H.D.P., B.F., and M.B. (Marco Borga); formal analysis, H.D.P.; investigation, H.D.P., B.F., and M.B. (Marco Borga); resources, M.Z.; data curation, H.D.P. and M.Z.; writing—original draft preparation, H.D.P., B.F., and M.B. (Marco Borga); writing—review and editing, H.D.P., B.F., M.B. (Marco Baratieri), C.B., M.Z., and M.B. (Marco Borga); visualization, H.D.P.; supervision, B.F. and M.B. (Marco Borga); All authors have read and agreed to the published version of the manuscript.

Funding: This research received no external funding.

Acknowledgments: The first author acknowledge the support from LPDP (Indonesia Endowment Fund for Education), Ministry of Finance, the Republic of Indonesia.

Conflicts of Interest: The authors declare no conflict of interest.

References

1. Virasjoki, V.; Siddiqui, A.S.; Zakeri, B.; Salo, A. Market Power With Combined Heat and Power Production in the Nordic Energy System. *IEEE Trans. Power Syst.* **2018**, *33*, 5263–5275. [CrossRef]
2. Sarıca, K.; Or, I. Efficiency assessment of Turkish power plants using data envelopment analysis. *Energy* **2007**, *32*, 1484–1499. [CrossRef]
3. Regulagadda, P.; Dincer, I.; Naterer, G.F. Exergy analysis of a thermal power plant with measured boiler and turbine losses. *Appl. Eng.* **2010**, *30*, 970–976. [CrossRef]
4. Çakir, U.; Çomakli, K.; Yüksel, F. The role of cogeneration systems in sustainability of energy. *Energy Convers. Manag.* **2012**, *63*, 196–202. [CrossRef]
5. Wang, H.; Yin, W.; Abdollahi, E.; Lahdelma, R.; Jiao, W. Modelling and optimization of CHP based district heating system with renewable energy production and energy storage. *Appl. Energy* **2015**, *159*, 401–421. [CrossRef]
6. Available online: http://www.code2-project.eu/wp-content/uploads/CODE-2-European-Cogeneration-Roadmap.pdf (accessed on 6 August 2020).
7. IPCC. Climate Change 2014: Mitigation of Climate Change. In *Contribution of Working Group III to the Fifth Assessment Report of the Intergovernmental Panel on Climate Change*; Edenhofer, O., Pichs-Madruga, R., Sokona, Y., Farahani, E., Kadner, S., Seyboth, K., Adler, A., Baum, I., Brunner, S., Eickemeier, P., et al., Eds.; Cambridge University Press: Cambridge, UK, 2014.
8. Moriarty, P.; Honnery, D. Can renewable energy power the future? *Energy Policy* **2016**, *93*, 3–7. [CrossRef]
9. Jäger-Waldau, A.; Kougias, I.; Taylor, N.; Thiel, C. How photovoltaics can contribute to GHG emission reductions of 55% in the EU by 2030. *Renew. Sustain. Energy Rev.* **2020**, *126*, 109836. [CrossRef]
10. Engeland, K.; Borga, M.; Creutin, J.-D.; François, B.; Ramos, M.-H.; Vidal, J.-P. Space-time variability of climate variables and intermittent renewable electricity production—A review. *Renew. Sustain. Energy Rev.* **2017**, *79*, 600–617. [CrossRef]
11. Staffell, I.; Pfenninger, S. The increasing impact of weather on electricity supply and demand. *Energy* **2018**, *145*, 65–78. [CrossRef]
12. Pérez Ciria, T.; Puspitarini, H.D.; Chiogna, G.; François, B.; Borga, M. Multi-temporal scale analysis of complementarity between hydro and solar power along an alpine transect. *Sci. Total Environ.* **2020**, *741*, 140179. [CrossRef]
13. Heide, D.; von Bremen, L.; Greiner, M.; Hoffmann, C.; Speckmann, M.; Bofinger, S. Seasonal optimal mix of wind and solar power in a future, highly renewable Europe. *Renew. Energy* **2010**, *35*, 2483–2489. [CrossRef]
14. von Bremen, L. *Large-Scale Variability of Weather Dependent Renewable Energy Sources*; Springer: Dordrecht, The Netherlands, 2010; pp. 189–206. [CrossRef]
15. François, B.; Borga, M.; Creutin, J.D.; Hingray, B.; Raynaud, D.; Sauterleute, J.F. Complementarity between solar and hydro power: Sensitivity study to climate characteristics in Northern-Italy. *Renew. Energy* **2016**, *86*, 543–553. [CrossRef]
16. François, B.; Hingray, B.; Raynaud, D.; Borga, M.; Creutin, J.D. Increasing climate-related-energy penetration by integrating run-of-the river hydropower to wind/solar mix. *Renew. Energy* **2016**, *87*, 686–696. [CrossRef]
17. Jurasz, J.; Ciapała, B. Integrating photovoltaics into energy systems by using a run-off-river power plant with pondage to smooth energy exchange with the power gird. *Appl. Energy* **2017**, *198*, 21–35. [CrossRef]
18. Ming, B.; Liu, P.; Cheng, L.; Zhou, Y.; Wang, X. Optimal daily generation scheduling of large hydro–photovoltaic hybrid power plants. *Energy Convers. Manag.* **2018**, *171*, 528–540. [CrossRef]
19. Raynaud, D.; Hingray, B.; François, B.; Creutin, J.D. Energy droughts from variable renewable energy sources in European climates. *Renew. Energy* **2018**, *125*, 578–589. [CrossRef]
20. Jurasz, J.; Canales, F.A.; Kies, A.; Guezgouz, M.; Beluco, A. A review on the complementarity of renewable energy sources: Concept, metrics, application and future research directions. *Sol. Energy* **2020**, *195*, 703–724. [CrossRef]

21. Beaudin, M.; Zareipour, H.; Schellenberglabe, A.; Rosehart, W. Energy storage for mitigating the variability of renewable electricity sources: An updated review. *Energy Sustain. Dev.* **2010**, *14*, 302–314. [CrossRef]
22. Hirth, L.; Ziegenhagen, I. Balancing power and variable renewables: Three links. *Renew. Sustain. Energy Rev.* **2015**, *50*, 1035–1051. [CrossRef]
23. Söder, L.; Lund, P.D.; Koduvere, H.; Bolkesjø, T.F.; Rossebø, G.H.; Rosenlund-Soysal, E.; Skytte, K.; Katz, J.; Blumberga, D. A review of demand side flexibility potential in Northern Europe. *Renew. Sustain. Energy Rev.* **2018**, *91*, 654–664. [CrossRef]
24. Romero Rodríguez, L.; Salmerón Lissén, J.M.; Sánchez Ramos, J.; Rodríguez Jara, E.Á.; Álvarez Domínguez, S. Analysis of the economic feasibility and reduction of a building's energy consumption and emissions when integrating hybrid solar thermal/PV/micro-CHP systems. *Appl. Energy* **2016**, *165*, 828–838. [CrossRef]
25. Salmerón Lissén, J.; Romero Rodríguez, L.; Durán Parejo, F.; Sánchez de la Flor, F. An Economic, Energy, and Environmental Analysis of PV/Micro-CHP Hybrid Systems: A Case Study of a Tertiary Building. *Sustainability* **2018**, *10*, 4082. [CrossRef]
26. Tan, S.; Wang, X.; Jiang, C. Optimal Scheduling of Hydro–PV–Wind Hybrid System Considering CHP and BESS Coordination. *Appl. Sci.* **2019**, *9*, 892. [CrossRef]
27. Daraei, M.; Avelin, A.; Thorin, E. Optimization of a regional energy system including CHP plants and local PV system and hydropower: Scenarios for the County of Västmanland in Sweden. *J. Clean Prod.* **2019**, *230*, 1111–1127. [CrossRef]
28. François, B.; Borga, M.; Anquetin, S.; Creutin, J.D.; Engeland, K.; Favre, A.C.; Hingray, B.; Ramos, M.H.; Raynaud, D.; Renard, B.; et al. Integrating hydropower and intermittent climate-related renewable energies: A call for hydrology. *Hydrol. Process.* **2014**, *28*, 5465–5468. [CrossRef]
29. GSE. *Rapporto delle Attivita 2018*; Gestore dei Servizi Energetici: Rome, Italy, 2019.
30. Patuzzi, F.; Prando, D.; Vakalis, S.; Rizzo, A.M.; Chiaramonti, D.; Tirler, W.; Mimmo, T.; Gasparella, A.; Baratieri, M. Small-scale biomass gasification CHP systems: Comparative performance assessment and monitoring experiences in South Tyrol (Italy). *Energy* **2016**, *112*, 285–293. [CrossRef]
31. Comodi, G.; Lorenzetti, M.; Salvi, D.; Arteconi, A. Criticalities of district heating in Southern Europe: Lesson learned from a CHP-DH in Central Italy. *Appl. Eng.* **2017**, *112*, 649–659. [CrossRef]
32. Gu, W.; Wang, J.; Lu, S.; Luo, Z.; Wu, C. Optimal operation for integrated energy system considering thermal inertia of district heating network and buildings. *Appl. Energy* **2017**, *199*, 234–246. [CrossRef]
33. Romanchenko, D.; Kensby, J.; Odenberger, M.; Johnsson, F. Thermal energy storage in district heating: Centralised storage vs. storage in thermal inertia of buildings. *Energy Convers. Manag.* **2018**, *162*, 26–38. [CrossRef]
34. Lundström, L.; Wallin, F. Heat demand profiles of energy conservation measures in buildings and their impact on a district heating system. *Appl. Energy* **2016**, *161*, 290–299. [CrossRef]
35. Christenson, M.; Manz, H.; Gyalistras, D. Climate warming impact on degree-days and building energy demand in Switzerland. *Energy Convers. Manag.* **2006**, *47*, 671–686. [CrossRef]
36. Lindelöf, D. Bayesian estimation of a building's base temperature for the calculation of heating degree-days. *Energy Build.* **2017**, *134*, 154–161. [CrossRef]
37. Ashfaq, A.; Kamali, Z.H.; Agha, M.H.; Arshid, H. Heat coupling of the pan-European vs. regional electrical grid with excess renewable energy. *Energy* **2017**, *122*, 363–377. [CrossRef]
38. Steinke, F.; Wolfrum, P.; Hoffmann, C. Grid vs. storage in a 100% renewable Europe. *Renew. Energy* **2013**, *50*, 826–832. [CrossRef]
39. Raj, N.T.; Iniyan, S.; Goic, R. A review of renewable energy based cogeneration technologies. *Renew. Sustain. Energy Rev.* **2011**, *15*, 3640–3648. [CrossRef]
40. Prina, M.G.; Cozzini, M.; Garegnani, G.; Manzolini, G.; Moser, D.; Oberegger, U.F.; Pernetti, R.; Vaccaro, R.; Sparber, W. Multi-objective optimization algorithm coupled to EnergyPLAN software: The EPLANopt model. *Energy* **2018**, *149*, 213–221. [CrossRef]
41. Frangopoulos, C.A. A method to determine the power to heat ratio, the cogenerated electricity and the primary energy savings of cogeneration systems after the European Directive. *Energy* **2012**, *45*, 52–61. [CrossRef]
42. Perpiñan, O.; Lorenzo, E.; Castro, M.A. On the calculation of energy produced by a PV grid-connected system. *Prog. Photovolt. Res. Appl.* **2007**, *15*, 265–274. [CrossRef]

43. Hänggi, P.; Weingartner, R. Variations in Discharge Volumes for Hydropower Generation in Switzerland. *Water Resour. Manag.* **2012**, *26*, 1231–1252. [CrossRef]
44. François, B.; Zoccatelli, D.; Borga, M. Assessing small hydro/solar power complementarity in ungauged mountainous areas: A crash test study for hydrological prediction methods. *Energy* **2017**. [CrossRef]
45. Norbiato, D.; Borga, M.; Merz, R.; Blöschl, G.; Carton, A. Controls on event runoff coefficients in the eastern Italian Alps. *J. Hydrol.* **2009**, *375*, 312–325. [CrossRef]
46. Zaramella, M.; Borga, M.; Zoccatelli, D.; Carturan, L. TOPMELT 1.0: A topography-based distribution function approach to snowmelt simulation for hydrological modelling at basin scale. *Geosci. Model. Dev.* **2019**, *12*, 5251–5265. [CrossRef]
47. Moore, R.J. The PDM rainfall-runoff model. *Hydrol. Earth Syst. Sci.* **2007**, *11*, 483–499. [CrossRef]
48. Puspitarini, H.D.; François, B.; Zaramella, M.; Brown, C.; Borga, M. The impact of glacier shrinkage on energy production from hydropower-solar complementarity in alpine river basins. *Sci. Total Environ.* **2020**, *719*, 137488. [CrossRef] [PubMed]
49. Hekkenberg, M.; Benders, R.M.J.; Moll, H.C.; Schoot Uiterkamp, A.J.M. Indications for a changing electricity demand pattern: The temperature dependence of electricity demand in the Netherlands. *Energy Policy* **2009**, *37*, 1542–1551. [CrossRef]
50. Chaudhary, P.; Rizwan, M. Voltage regulation mitigation techniques in distribution system with high PV penetration: A review. *Renew. Sustain. Energy Rev.* **2018**, *82*, 3279–3287. [CrossRef]
51. Moshövel, J.; Kairies, K.P.; Magnor, D.; Leuthold, M.; Bost, M.; Gährs, S.; Szczechowicz, E.; Cramer, M.; Sauer, D.U. Analysis of the maximal possible grid relief from PV-peak-power impacts by using storage systems for increased self-consumption. *Appl. Energy* **2015**, *137*, 567–575. [CrossRef]
52. Zhang, Y.; Campana, P.E.; Lundblad, A.; Yan, J. Comparative study of hydrogen storage and battery storage in grid connected photovoltaic system: Storage sizing and rule-based operation. *Appl. Energy* **2017**, *201*, 397–411. [CrossRef]
53. François, B.; Hingray, B.; Borga, M.; Zoccatelli, D.; Brown, C.; Creutin, J.-D. Impact of Climate Change on Combined Solar and Run-of-River Power in Northern Italy. *Energies* **2018**, *11*, 290. [CrossRef]
54. Tafarte, P.; Kanngießer, A.; Dotzauer, M.; Meyer, B.; Grevé, A.; Millinger, M. Interaction of Electrical Energy Storage, Flexible Bioenergy Plants and System-friendly Renewables in Wind- or Solar PV-dominated Regions. *Energies* **2020**, *13*, 1133. [CrossRef]
55. Gast, N.; Tomozei, D.-C.; Le Boudec, J.-Y. Optimal Generation and Storage Scheduling in the Presence of Renewable Forecast Uncertainties. *IEEE Trans. Smart Grid.* **2014**, *5*, 1328–1339. [CrossRef]
56. Craparo, E.; Karatas, M.; Singham, D.I. A robust optimization approach to hybrid microgrid operation using ensemble weather forecasts. *Appl. Energy* **2017**, *201*, 135–147. [CrossRef]
57. Liu, K.; Hu, X.; Yang, Z.; Xie, Y.; Feng, S. Lithium-ion battery charging management considering economic costs of electrical energy loss and battery degradation. *Energy Convers. Manag.* **2019**, *195*, 167–179. [CrossRef]
58. Ouyang, Q.; Wang, Z.; Liu, K.; Xu, G.; Li, Y. Optimal Charging Control for Lithium-Ion Battery Packs: A Distributed Average Tracking Approach. *IEEE Trans. Ind. Inform.* **2020**, *16*, 3430–3438. [CrossRef]
59. Liu, K.; Zou, C.; Li, K.; Wik, T. Charging Pattern Optimization for Lithium-Ion Batteries With an Electrothermal-Aging Model. *IEEE Trans. Ind. Inform.* **2018**, *14*, 5463–5474. [CrossRef]
60. GSE. *Rapporto Statistico Energia da Fonti Renovabili in Italia Anno 2016*; Gestore dei Servizi Energetici: Rome, Italy, 2018.
61. Silvestro, F.; Parodi, A.; Campo, L.; Ferraris, L. Analysis of the streamflow extremes and long-term water balance in the Liguria region of Italy using a cloud-permitting grid spacing reanalysis dataset. *Hydrol. Earth Syst. Sci.* **2018**, *22*, 5403–5426. [CrossRef]
62. Weitemeyer, S.; Kleinhans, D.; Vogt, T.; Agert, C. Integration of Renewable Energy Sources in future power systems: The role of storage. *Renew. Energy* **2015**, *75*, 14–20. [CrossRef]
63. Heide, D.; Greiner, M.; von Bremen, L.; Hoffmann, C. Reduced storage and balancing needs in a fully renewable European power system with excess wind and solar power generation. *Renew. Energy* **2011**, *36*, 2515–2523. [CrossRef]
64. Pääkkönen, A.; Joronen, T. Revisiting the feasibility of biomass-fueled CHP in future energy systems—Case study of the Åland Islands. *Energy Convers. Manag.* **2019**, *188*, 66–75. [CrossRef]

65. Wei, J.; Zhang, Y.; Wang, J.; Cao, X.; Khan, M.A. Multi-period planning of multi-energy microgrid with multi-type uncertainties using chance constrained information gap decision method. *Appl. Energy* **2020**, *260*, 114188. [CrossRef]
66. Li, Q.; Wang, J.; Zhang, Y.; Fan, Y.; Bao, G.; Wang, X. Multi-period generation expansion planning for sustainable power systems to maximize the utilization of renewable energy sources. *Sustainability* **2020**, *12*, 1083. [CrossRef]
67. Chowdhury, N.; Pilo, F.; Pisano, G. Optimal energy storage system positioning and sizing with robust optimization. *Energies* **2020**, *13*, 512. [CrossRef]